2018 EAGE ANNUAL
80TH CONFERENCE + EXHIBITION
COPENHAGEN | DENMARK

We D 16

Systematic Detection and Correction of Instrument-Related Time Shifts Using Seismic Interferometric Surface Waves

J. De Laat* (Utrecht University, KNMI), C. Weemstra (KNMI, Delft University of Technology), A. Verdel (TNO), P. Jousset (GFZ), G. Páll Hersir (ISOR), H. Blanck (ISOR)

Summary

Timing errors are a notorious problem in seismic data acquisition and processing. A technique is presented that allows such time shifts to be detected and corrected in a systematic fashion. The methodology relies on virtual-source responses retrieved through the application of seismic interferometry (SI). In application to recordings of ambient seismic noise, SI involves temporal averaging of time-windowed crosscorrelation measurements. Because surface waves dominate the ambient seismic field, the retrieved interferometric responses are typically also dominated by surface waves. Under favorable conditions, these interferometric responses therefore approach the surface-wave part of the medium's Green's function. Additionally, however, its time-reverse is also retrieved under those conditions. This implies time-symmetry of the time-averaged receiver-receiver crosscorrelations. It is this time-symmetry that is exploited in this study. By comparing the arrival time of the interferometric surface waves at positive time to the arrival time of the interferometric surface waves at negative time for a large a number of receiver-receiver pairs, relative timing errors are determined in a least-squared sense. The proposed methodology is validated using both synthetic data and field data. The results hold particular promise for time-lapse (4D) seismic surveys.

Introduction

Seismic interferometry (SI) allows one to generate new seismic responses by crosscorrelating observations at different receiver locations (Wapenaar et al. (2010)). In application to recordings of ambient seismic noise, SI involves temporal averaging of time-windowed crosscorrelation measurements (e.g., Weemstra et al. (2013)). The retrieved interferometric responses are typically dominated by surface waves (e.g., de Ridder and Biondi (2013)). Time-averaged crosscorrelations therefore often approach the surface-wave part of the medium's Green's function (Wapenaar et al. (2010)). Assuming a uniform illumination pattern, the Green's function's time-reverse is additionally retrieved, implying time-symmetry of the time-averaged receiver-receiver crosscorrelations. By comparing the arrival time of the interferometric surface waves at positive time to the arrival time of the interferometric surface waves at negative time, this time-symmetry can be exploited for the purpose of estimating relative timing errors (e.g., Sens-Schönfelder (2008)). We show that by doing this in a least-squares sense for a large a number of receiver-receiver pairs using both synthetic data and field data of the Reykjanes seismis array (RARR).

The Reykjanes seismic array

This study is motivated by the recent deployment of the RARR (Weemstra et al. (2016)). The RARR is a composite array centered around the tip of the Reykjanes peninsula, SW Iceland (Figure 1). The backbone of this array consists of 56 stations deployed in the context of IMAGE (Integrated Methods for Advanced Geothermal Exploration), including 23 locations sampled by ocean bottom seismometers (OBSs). One of the main objectives of the IMAGE seismic campaign is to assess the potential of SI in the context of geothermal exploration. The application of seismic tomography, and hence the extraction of receiver-receiver phase (or group) velocities from the retrieved virtual-source responses, is of particular interest. The accuracy of these receiver-receiver phase velocities, and hence the derived tomographic maps, is strongly dependent on the accuracy of the timing of the exploited noise recordings. This temporal accuracy and stability, however, cannot always be guaranteed. For example, the absence of a GPS connection of the OBSs may result in so-called clock time drift (Shariat-Panahi et al. (2009)).

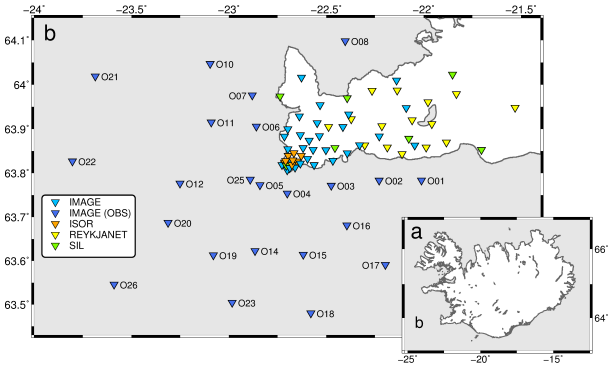

Figure 1 *a) Relative location of the RARR and, b) the configuration of this composite array. Different colors indicate different networks/deployments.*

Theory

Let us consider two surface receivers located at $\mathbf{x}_i$ and $\mathbf{x}_j$, with the azimuth of the vector pointing from $\mathbf{x}_i$ to $\mathbf{x}_j$ denoted by $\theta_{i,j}$ (measured counter clockwise from North). Under the assumption that i) the noise sources illuminate the station couple uniformly from all angles, ii) the sources have coinciding amplitude spectra and that iii) the medium is lossless, the ensemble-averaged cross-correlation will be proportional to the Green's function plus its time reversed, convolved with the auto-correlation of the signal emitted by the noise sources (Wapenaar and Fokkema (2006)). An additional condition should be fulfilled in order to correctly retrieve the surface-wave part of the Green's function from surface-wave noise: the ambient seismic noise field should be dominated by a single surface-wave mode (Halliday and Curtis (2008)).

In case all above-mentioned conditions are fulfilled, the time-averaged crosscorrelation of the noise recorded by receivers $\mathbf{x}_i$ and $\mathbf{x}_j$ will contain a peak at positive time (commonly referred to as the 'causal part') and a peak at negative time (the 'a-causal part'), whose times of arrival we denote by $t_{i,j}^{(+)}$ and $t_{i,j}^{(-)}$, respectively. The arrival at $t_{i,j}^{(+)}$ represents the surface wave at x_j due to a virtual source at x_i, whereas the arrival at $t_{i,j}^{(-)}$ represents the surface wave at x_i due to a virtual source at x_j. Source-receiver reciprocity

implies that $t_{i,j}^{(+)} = -t_{i,j}^{(-)}$ (Wapenaar and Fokkema (2006)). In case the recordings by receiver i are subject to timing errors, this will add a time shift of $\delta t_i^{(\mathrm{ins})}$ to the observed arrival time. Here, a negative value of $\delta t_i^{(\mathrm{ins})}$ implies that the recordings by receiver i are subject to a time delay. Accounting for these time shifts, summing the observed arrival time at positive and negative time (denoted by $t_{i,j}^{(-,\mathrm{obs})}$ and $t_{i,j}^{(+,\mathrm{obs})}$, respectively) gives:

$$t_{i,j}^{(+,\mathrm{obs})} + t_{i,j}^{(-,\mathrm{obs})} = 2\delta t_i^{(\mathrm{ins})} - 2\delta t_j^{(\mathrm{ins})}. \tag{1}$$

Note that the travel times associated with the medium (i.e., $t_{i,j}^{(+)}$ and $t_{i,j}^{(-)}$) are absent in this equation because they cancel.

Extending this to a total of N simultaneous recording receivers, we obtain the matrix equation:

$$\mathbf{T}^{(\mathrm{obs})} = \mathbf{A}\mathbf{T}^{(\mathrm{ins})}, \tag{2}$$

where the rows and columns of matrix $\mathbf{A}$ relate to different receiver pairs and receivers, respectively. Each row of A will thus only contain two non-zero entries: 2 and -2 (associated with $\delta t_i^{(\mathrm{ins})}$ and $\delta t_j^{(\mathrm{ins})}$, respectively). The column vector $\mathbf{T}^{(\mathrm{ins})}$ holds the N instrument-related time shifts we aim to estimate. If we can estimate $t_{i,j}^{(+,\mathrm{obs})}$ and $t_{i,j}^{(-,\mathrm{obs})}$ for all receiver pairs, the matrix $\mathbf{A}$ will contain $N(N-1)/2$ rows. However, in reality this number will be smaller as $t_{i,j}^{(+,\mathrm{obs})}$ and/or $t_{i,j}^{(-,\mathrm{obs})}$ can generally not be determined for all receiver couples i and j.

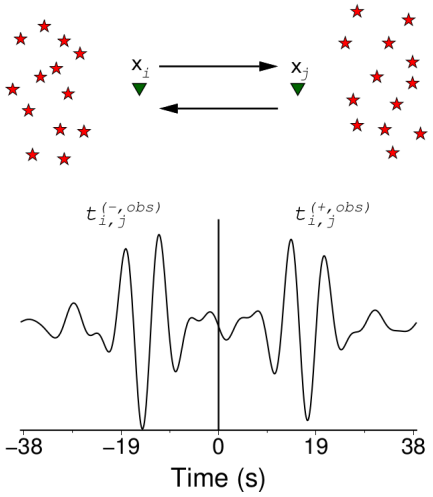

Figure 2 *Schematic representation of the causal and a-causal part of the time-averaged cross-correlation.*

The least-squares estimator of $\mathbf{T}^{(\mathrm{ins})}$, which we denote by $\widetilde{\mathbf{T}}^{(\mathrm{ins})}$, is given by

$$\widetilde{\mathbf{T}}^{(\mathrm{ins})} = \left(\mathbf{A}^T\mathbf{A}\right)^{-1}\mathbf{A}^T\mathbf{T}^{(\mathrm{obs})}. \tag{3}$$

As it stands, the system of equations (2) is under-determined. ($\mathbf{A}$ is rank deficient with its rank always being one lower than the number of receivers N). In other words, an infinite number of combinations of the time shifts $\widetilde{\delta t}_i^{(\mathrm{ins})}$ ($i = 1,...,N$) exist that minimize the least-squares error. In case one or more of the N receivers are devoid of instrument-related time shifts, however, the appropriate least-squares solution can be obtained by imposing the additional constraint:

$$\min_{\widetilde{\delta t}_i^{(\mathrm{ins})}} \sum_{\substack{i=1 \\ \delta t_i^{(\mathrm{ins})}=0}}^{N} \left(\widetilde{\delta t}_i^{(\mathrm{ins})} - \delta t_i^{(\mathrm{ins})}\right)^2. \tag{4}$$

The time-symmetry of the time-averaged crosscorrelations is strictly valid under the assumption of a uniform illumination pattern. In practice, however, the energy flux of the surface-wave noise often varies as a function of azimuth (e.g., Weemstra et al. (2013)). We account for this deviation from a uniform illumination by introducing the additional time shifts $\delta t_{i,j}^{(+,\mathrm{src})}$ and $\delta t_{i,j}^{(-,\mathrm{src})}$, which represent (source-related) time delays of the causal and a-causal arrivals, respectively. Illumination-related time shifts have previously been ignored in similar studies (e.g., Sens-Schönfelder (2008)). Including these time shifts in our model gives,

$$t_{i,j}^{(+,\mathrm{obs})} + t_{i,j}^{(-,\mathrm{obs})} = 2\delta t_i^{(\mathrm{ins})} - 2\delta t_j^{(\mathrm{ins})} + \delta t_{i,j}^{(+,\mathrm{src})} + \delta t_{i,j}^{(-,\mathrm{src})}. \tag{5}$$

Again extending this to a total of N simultaneously recording receivers gives,

$$\mathbf{T}^{(\mathrm{obs})} = \mathbf{A}\mathbf{T}^{(\mathrm{ins})} + \mathbf{T}^{(\mathrm{src})}, \tag{6}$$

where $\mathbf{T}^{(\mathrm{src})}$ contains the $\delta t_{i,j}^{(+,\mathrm{src})} + \delta t_{i,j}^{(-,\mathrm{src})}$. A stationary-phase approximation of $\delta t_{i,j}^{(+,\mathrm{src})} + \delta t_{i,j}^{(-,\mathrm{src})}$ is derived by Weaver et al. (2009). Assuming a sufficiently smooth illumination pattern, these authors find:

$$\delta t_{i,j}^{(+,\mathrm{src})} + \delta t_{i,j}^{(-,\mathrm{src})} \sim \frac{B\text{''}(\theta_{i,j})}{2t_{i,j}\omega_0^2 B(\theta_{i,j})} - \frac{B\text{''}(\theta_{i,j}-180)}{2t_{i,j}\omega_0^2 B(\theta_{i,j}-180)}, \tag{7}$$

where $B(\theta)$ denotes the power of the noise flux as a function of azimuth, t the traveltime between the virtual source and the receiver and ω_0 the central angular frequency of the correlation waveform (Weaver et al. (2009)). Using this approximation, the weighted least-squares solution to equation 6 reads:

$$\widetilde{\mathbf{T}}^{(\mathrm{ins})} = \left(\mathbf{A}^T\mathbf{W}_\mathrm{d}\mathbf{A}\right)^{-1}\mathbf{A}^T\mathbf{W}_\mathrm{d}\mathbf{T}^{(\mathrm{obs})}. \tag{8}$$

The weight matrix $\mathbf{W}_\mathrm{d}$ is a diagonal matrix whose dimension coincides with the number of observations (i.e., with the length of $\mathbf{T}^{(\mathrm{obs})}$). The weight factors (diagonal elements) are given by the inverse of equation 7 for each station couple i and j. In case $B(\theta_{i,j})$ and $t_{i,j}$ are not known, which, in application to time-averaged crosscorrelations of ambient seismic noise, is often the case, the weighting can be simplified by approximating the inverse of equation 7 by the receiver-receiver distance $|\mathbf{x}_j - \mathbf{x}_i|$.

Results synthetic data

We created two synthetic data sets, each consisting of four months of (hourly) synthetic seismic noise recordings of single-mode dispersive surface-waves (e.g, Halliday and Curtis (2008)). The first data set is the result of a uniform illumination by uncorrelated plane waves from all angles, whereas the second set of synthetic recordings is due to uncorrelated plane waves associated with an arbitrary (but smooth) non-uniform illumination pattern. In both cases, the OBS recordings were given an arbitrary (constant) clock time error between -2 and 2 s. Time-averaged crosscorrelations were created by summing the individual hourly crosscorrelations. Although the synthetic data contained energy between 0.05 and 0.5 Hz, the time-averaged crosscorrelation were filtered between 0.09 and 0.27 Hz. By crosscorrelating the (spline-interpolated) causal and a-causal arrivals, $\delta t_{i,j}^{(+,\mathrm{obs})} + \delta t_{i,j}^{(-,\mathrm{obs})}$ was obtained for each receiver couple (i,j).

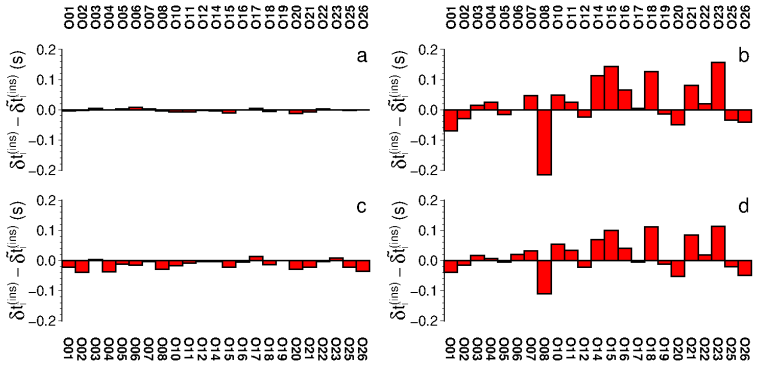

Figure 3 *Residual error ($\delta t_i^{(\mathrm{ins})} - \widetilde{\delta t}_i^{(\mathrm{ins})}$) for every OBS for a) uniform illumination, b) non-uniform illumination without weighing factors, c) with equation 7 as weighing factors and d) with receiver-receiver distance as weighing factors.*

Figures 3a) and b) give the errors after applying equation 3 to the time-averaged crosscorrelations of over 600 receiver-receiver couples associated with a uniform and a non-uniform illumination, respectively. Figure 3c) gives the residual error using equation 8 instead. The weighted inversion reduces the residual errors to values below 0.04s. The remaining errors can be attributed to spurious traveltime delays due to (remaining) constructive interference of uncorrelated signal associated with different noise sources (e.g., Weemstra et al. (2014)). Figure 3d) shows the error when equation 3 is weighted only by the receiver-receiver distance. Although the residual error has decreased relative to figure 3b), a significant error remains, substantiating the importance of the effect of the illumination pattern $B(\theta)$.

Results field data

Assuming the land IMAGE receivers to be devoid of instrument-related time shifts, we obtained the instrument-related time shifts for all 86 receivers of the RARR, based on the time-averaged crosscorrelations of 650 couples (Figure 4). As the illumination pattern $B(\theta)$ is unknown, this result is a first order estimate using only the inverse of the receiver-receiver distance to weight the inversion. A thorough interpretation of the timing errors in Figure 4 requires more analysis. In particular, a potential bias of the obtained $\widetilde{\delta t}_i^{(\mathrm{ins})}$ due to deviation from zero of the mean of the $t_{i,j}^{(+,\mathrm{obs})} + t_{i,j}^{(-,\mathrm{obs})}$ needs to be investigated. This will be the subject of (near) future research.

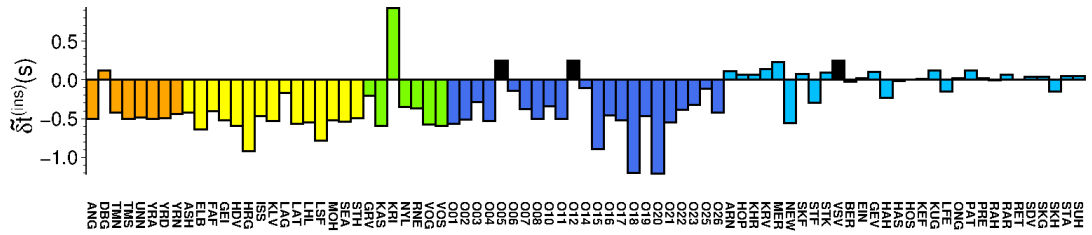

Figure 4 *The computed instrument-related time shift, $\widetilde{\delta t}_i^{(\mathrm{ins})}$, obtained for the field data of the RARR. Colors refer to the networks/deployments as given in Figure 1.*

Conclusions

We have derived a formulation that allows interferometric surface-wave responses to be exploited for the purpose of detecting timing errors. We validated the method using synthetic surface-wave (noise) recordings and applied it to field data recorded on and around the Reykjanes peninsula, SW Iceland. The technique could be useful in a variety of seismic (ocean bottom) contexts.

Acknowledgments

We are grateful to the institute of geophysics of the Czech acadamy of sciences (CAS) for using the data recorded by the REYKJANET stations. Similarly, we thank the Icelandic meteorological office (MET office) for allowing us to use their data (SIL network). Instruments for the IMAGE project were provided by the Geophysical Instrument pool Potsdam and the German instrument pool for amphibian seismology. The research leading to these results has received funding from the European Community's Seventh Framework Programme under grant agreement No. 608553 (Project IMAGE).

References

Halliday, D. and Curtis, A. [2008] Seismic interferometry, surface waves and source distribution. *Geophysical Journal International*, **175**(3), 1067–1087.

de Ridder, S.A.L. and Biondi, B.L. [2013] Daily reservoir-scale subsurface monitoring using ambient seismic noise. *Geophysical Research Letters*, **40**, 1–6.

Sens-Schönfelder, C. [2008] Synchronizing seismic networks with ambient noise. *Geophysical Journal International*, **174**(3), 966–970.

Shariat-Panahi, S., Alegria, F.C., Làzaro, A.M. and del Rio, J. [2009] Time Drift of Ocean Bottom Seismometers (Obs). In: *Proceedings of the 19th IMEKO World Congress on Fundamental and Applied Metrology*. 2548–2553.

Wapenaar, C., Draganav, D., Snieder, R., Campman, X. and Verdel, A. [2010] Tutorial on seismic interferometry: Part 1 - Basic principles and applications. *Geophysics*, **75**(5), 75A195 – 75A209.

Wapenaar, K. and Fokkema, J. [2006] Green's function representations for seismic interferometry. *Geophysics*, **71**(4), SI33–SI46.

Weaver, R., Froment, B. and Campillo, M. [2009] On the correlation of non-isotropically distributed ballistic scalar diffuse waves. *The Journal of the Acoustical Society of America*, **126**(4), 1817–1826.

Weemstra, C., Boschi, L., Goertz, A. and Artman, B. [2013] Seismic attenuation from recordings of ambient noise. *Geophysics*, **78**(1), Q1–Q14.

Weemstra, C., Obermann, A., Verdel, A., Paap, B., Blanck, H., Gusnason, E.Á., Hersir, G.P., Jousset, P. and Sigurdsson, Ó. [2016] Time-lapse seismic imaging of the Reykjanes geothermal reservoir. In: *Proceedings of the European Geothermal Congress*. European Geothermal Energy Council (EGEC), Strassbourg.

Weemstra, C., Westra, W., Snieder, R. and Boschi, L. [2014] On estimating attenuation from the amplitude of the spectrally whitened ambient seismic field. *Geophysical Journal International*, **197**, 1770–1788.